Water-jet Propelled Autonomous Surface Vehicle UCAP: System Description and Control

Bruno M. Ferreira*, Aníbal C. Matos*†, José C. Alves*†
* INESC TEC
† Faculty of Engineering, University of Porto
FEUP Campus
Rua Dr. Roberto Frias
4200-465 Porto, Portugal
bm.ferreira@fe.up.pt

***Abstract*—A new small-sized autonomous surface vehicle actuated by a water-jet has been developed at INESC TEC for search and rescue of victims at sea. This paper describes the vehicle main components and presents the control and guidance laws governing the motion and enabling it to perform line-following and target tracking missions. Results from field trials are presented, demonstrating the capabilities and the performances of the vehicle along with its control layer.**

I. Introduction

Autonomous marine robots are gaining importance in several coastal and offshore applications. Sound examples include persistent surveillance, environmental data harvesting, search and rescue. This latter is the main focus of the FP7 European project integrated components for assisted rescue and unmanned search operations (ICARUS), which involves institutions from ten countries. Among many other contributions, INESC TEC contributed with the development of an unmanned surface vehicle – unmanned capsule (UCAP) – (Fig. 1) for rescuing victims at sea. For the search and rescue operations considered in the ICARUS project, the UCAP is intended to be small and lightweight. This vehicle should be capable to navigate at sea and and to carry a life raft.

In a typical mission, the UCAP should be capable to navigate according to assigned tasks, which include waypoint-based navigation or target-tracking. This paper describes the system and presents a control approach for this nonholonomic vehicle. The results obtained during field experiments are also be presented.

Related work

Related projects have proposed robotic tools for search and rescue at sea. Sound examples include AGAPAS (Autonomous Galileo-Supported Rescue Vessel for Persons Overboard) and EMILY (EMergency Integrated Lifesaving lanYard). The AGAPAS is a project orientated specifically to person overboard situations, where an automatic system perceives that someone fell from the vessel and deploys a USV capable of fetching that person [1]. The EMILY is a remotely operated/autonomous vessel that aims to assist the lifeguards in crowded beaches, providing them a safe and fast response mean [2].

II. System requirements

The main requirements of the UCAP were established taking into account a typical rescue operation at sea. The vehicle should be capable of navigating for at least $20\,\mathrm{min}$ at a minimum velocity of $1\,\mathrm{m\,s^{-1}}$, being also able to carry an inflatable life raft. The vehicle should represent little risks for humans during rescue operations, while being sufficiently robust to be deployed from other vessels and navigating in harsh conditions. Table I summarizes the main requirements for the UCAP.

TABLE I
UCAP requirements

Parameter	Value
Max. length	$1.5\,\mathrm{m}$
Max. width	$0.5\,\mathrm{m}$
Max. weight	$45\,\mathrm{kg}$
Speed	at least $1\,\mathrm{m\,s^{-1}}$
Payload capacity	capable to carry a life-raft for 4 people

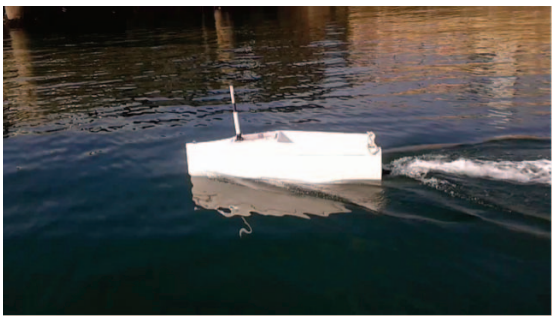

Fig. 1. Unmanned capsule (UCAP)

978-1-4673-9724-7/16/$31.00 ©2016 IEEE

III. System description

Apart from the hull, that was adapted from the autonomous sailboat FASt [3], the remaining elementary components have been designed in a modular fashion. The basic set of electronics, energy storage and actuation were thought as separated modules, enabling easy replacement of these components and different combinations of power, computing devices or sensors.

A. Body

The vehicle's hull has $1.5\,\mathrm{m}$ of length and weights approximately $25\,\mathrm{kg}$ with no payload. The body was designed so that it represents minimal risk for potential victims at sea as it should be capable to reach clusters of human victims in disaster scenarios. Therefore, the vehicle was intended to be relatively lightweight. Simultaneously, the UCAP is also intended to be robust enough to be carried on and released from other surface vehicles at sea and to navigate in harsh conditions. The body is entirely made of fiberglass, containing two main volumes: a dry compartment at bow where the computational system and sensors, are placed in; and a wet deck intended to carry additional payload. This open volume is especially relevant in the context of the ICARUS project as it provides room for life rafts or life jackets.

B. Power

The UCAP is powered by a lithium polymer battery pack with a capacity of $220\,\mathrm{W\,h}$, enabling rescue operations lasting up to one hour at $1\mathrm{m\,s^{-1}}$. A digital controller was developed to monitor the discharge of the batteries and to protect them against overcurrent. The controller is configurable and can be set according to the requirements of the application. High current (up to $40\,\mathrm{A}$) and medium current (up to $10\,\mathrm{A}$) connectors are provided to actuation and electronics, respectively. Additionally, it also includes a connector for battery charging and balancing and a USB connection for status feedback.

C. Electronics & communications

The minimal set of electronics includes a computer, a communication access point, voltage regulators, an inertial measurement unit (IMU) and a GPS receiver. The electronics module is composed of a central computer interfacing with sensors and actuators over standard serial communications. In order to meet supply requirements of the different components, the electronics module regulates battery voltage to three different levels. In its basic configuration, the UCAP electronics module include an IMU to feed the navigation algorithms with angles and angular velocity measurements and a GPS device providing absolute position and linear velocity.

A WiFi access point repeater at $2.4\,\mathrm{GHz}$ provides remote connection to the on-board computer A $6\,\mathrm{dBi}$ omni-directional antenna is used making this combination capable of providing a reliable link at several hundreds of meters.

D. Actuation

At the stern, a water-jet module, actuated by a brushless motor, generates thrust to drive the UCAP to a maximum speed of $2\,\mathrm{m\,s^{-1}}$. This solution has been designed with the safety of victims in mind and also to facilitate launching from a mother vessel. The absence of harmful mechanisms such as unprotected rotating propellers makes it a suitable choice for rescue applications. The power delivered to the motor has been limited by software to approximately $450\,\mathrm{W}$, enabling a bollard thrust up to $5\,\mathrm{kg}$. A directional nozzle, whose angle is actuated by a servomotor, guides the jet to create a moment on the z-axis of the vehicle. Locally, a microprocessor monitors the performances and commands the brushless motor and the servomotor, according to the requests sent by the central computer, providing relevant measurements upstream, such as voltage and current consumption.

IV. Control

The control approach relies on an inner-outer loop controller designed for marine vehicle. This type of controller has already been applied to several robots [4], [5], with different thrust configuration, having performances demonstrated over tens of missions accomplished so far. The adaptation of the controller to the UCAP specific case will be detailed. In particular, the controller parametrizable nature will be explored and the actuation forces and moments will be modelled to build a new, specific controller for this vehicle.

At the guidance level, the UCAP will be able to perform line-following maneuvers defined by consecutive waypoints. Moreover, a target-tracking guidance law will be presented. This type of maneuver has already been applied to other surface vehicles with two decoupled degrees of freedom (DOFs) with positioning errors of approximately $20\,\mathrm{cm}$. The challenge with the UCAP is that the DOFs cannot be decoupled as a rotation on the vertical axis requires forward thrust.

A. Dynamics

Define the vehicle's pose as $\eta(t) = [\eta_l(t)^T \ \eta_a(t)^T]^T \in \mathbb{R}^6$, expressed in an inertial, earth-fixed referential $\{\mathcal{I}\}$, where $\eta_l(t) = [x(t) \ y(t) \ z(t)]^T$ is the vector of linear three-dimensional position and $\eta_a(t) = [\phi(t) \ \theta(t) \ \psi(t)]^T$ is the vector of roll, pitch and yaw angles.

A vehicle-fixed referential $\{\mathcal{B}\}$ was also considered, with regard to which the linear and angular velocities of the vehicle are expressed, as follows: $\nu(t) = [\nu_l(t) \ \nu_a(t)]$, where $\nu_l(t) = [u(t) \ v(t) \ w(t)]^T$ is the vector of linear surge, sway and heave velocities and $\nu_a(t) = [p(t) \ q(t) \ r(t)]$ is the vector of angular rolling, pitching and yawing velocities, respectively. In marine environments, drifts commonly resulting from winds and currents impact on the vehicle position. That is usually modelled by the inclusion of a drift velocity $\nu_d(t)$, expressed in the earth-fixed frame $\{\mathcal{I}\}$ and we consider that it is irrotational, which means that its angular components are null.

The pose vector time derivative and the body-expressed velocity are related though the following expression:

$$\dot{\eta} = J(\eta_a(t))\nu + \nu_d(t), \tag{1}$$

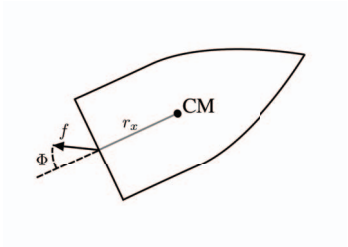

Fig. 2. Water-jet and nozzle direction

where $J(\eta_a(t))$ is a mapping function between the frames $\{\mathcal{B}\}$ and $\{\mathcal{I}\}$, which can be decomposed as follows:

$$J(\eta_a(t)) = \begin{bmatrix} J_l(\eta_a(t)) & \mathbf{0}_{3\times 3} \\ \mathbf{0}_{3\times 3} & J_a(\eta_a(t)) \end{bmatrix}. \tag{2}$$

For further details on these matrices, the reader is referred to [6].

The dynamics of a vehicle can be generically described by the nonlinear differential equation

$$M\dot{\nu} = A(\nu)\nu - g(\eta) + T\tau, \tag{3}$$

where $M \in \mathbb{R}^{6\times 6}$ is the added mass and inertia matrix, the matrix $A \in \mathbb{R}^{6\times 6}$ results from the hydrodynamic forces applied on the body of the vehicle when it is moving at a velocity ν. The term $A(\nu)\nu$ constitute the effect of added mass, Coriolis, centriptal and viscous damping forces and moments. The vector $g \in \mathbb{R}^6$ includes the effects of the restoring forces and moments, while $T \in \mathbb{R}^{6\times 2}$, with is a constant matrix that maps the forces and moments created by the actuators, whose actuation forces are given in the vector $\tau \in \mathbb{R}^2$, in the body-fixed reference frame.

For the particular case of the UCAP, τ comes as a function of the nozzle direction Φ (see Fig. 2) and of the actual force exerted by the water-jet and is given by

$$\tau = \begin{bmatrix} \tau_1 \\ \tau_2 \end{bmatrix} = \begin{bmatrix} f\cos\Phi \\ f\sin\Phi \end{bmatrix}.$$

T and is defined as

$$T = \begin{bmatrix} 1 & 0 \\ 0 & 1 \\ 0_{3\times 1} & 0_{3\times 1} \\ 0 & -r_x \end{bmatrix}$$

where r_x is the x-coordinate of the point of force application of the water-jet, expressed in the body-fixed coordinate system.

B. Inner loop

Based on (3), consider the reduced order velocity vector $\bar{\nu}(t) : \mathbb{R} \to \mathbb{R}^n$, whose dynamics is given by

$$\dot{\bar{\nu}}(t) = PM^{-1}\left(A(\nu)\nu - g(\eta) + T\tau\right), \tag{4}$$

where the reduced order matrices and vectors are given by

$$\bar{\nu}(t) = P\nu(t),$$

with $P \in R^{n\times 6}$ being a projection matrix defined as follow:

$$P = \begin{bmatrix} 1 & 0_{1\times 4} & 0 \\ 0 & 0_{1\times 4} & 1 \end{bmatrix}.$$

This matrix maps the overall system in a smaller dimension subspace considering only the relevant DOFs, by selecting the corresponding rows and columns. Notice that the product $PM^{-1}T$ has full rank.

In order to find a suitable control law, define the desired velocity vector as $\nu^*(t) \in \mathbb{R}^2$ and the velocity error vector as:

$$\tilde{\nu}(t) = \bar{\nu}(t) - \nu^*(t),$$

which one desire to reduce to zero. The reference vector $\nu^*(t)$ is composed of the surge and yaw velocity components.

Hence, the control law is chosen as

$$\tau^* = \left(PM^{-1}T\right)^{-1} \cdot \left(PM^{-1}(A(\nu)\nu - g(\eta)) + \dot{\nu}^*(t) - K_\nu\tilde{\nu}(t)\right). \tag{5}$$

This control law projects a desired virtual actuation τ. The actual inputs f and Φ are then computed as follows:

$$\begin{cases} f^* = \tau_1^*/\cos\Phi \\ \Phi^* = \operatorname{atan}(\tau_2^*/\tau_1^*) \end{cases}, \tag{6}$$

assuming that Φ and f vary instantaneously, which is a mild assumption considering that their dynamics is much faster than the vehicle dynamics. Note that f is always defined since the angle Φ is constrained to lie in an interval $\Phi \in [-\overline{\Phi}, \overline{\Phi}]$, $\overline{\Phi} < \pi/2$ due to mechanical constraints.

C. Outer loop

Line-following and target-tracking guidance laws are presented thereafter. These two guidance laws provide versatility to accomplish several types of missions composed of waypoints or trajectories defined by splines, for example.

From the control law in (5), one can assume that the velocity is controlled directly by setting $\nu^*(t) = [u^*\ r^*]^T$, where u^* and r^* represent the desired surge and yaw velocities.

1) Line-following: For line-following maneuvers, surge can be set independently of the yaw rate. Usually surge is set strictly positive and constant while the angular velocity is given by

$$r^* = K_L\left((\psi_l - \psi) + \xi(\psi_l, \eta)\right), \tag{7}$$

where the first term is meant to align the vehicle with the line heading ψ_l, $K_L > 0$ is constant gain and $\xi(\psi_l, \eta)$ is a function of the cross-track error which is given as

$$\xi = \operatorname{asin}\left(\operatorname{sat}\left(K_c u^* e_c,\ 1\right)\right).$$

The function $\operatorname{sat}(\cdot,\ \cdot)$ is a simple saturation function defined as follows

$$\operatorname{sat}(\alpha,\ \overline{\alpha}) = \begin{cases} \alpha & \text{if } |\alpha| \le \overline{\alpha} \\ \overline{\alpha}\frac{\alpha}{|\alpha|} & \text{if } |\alpha| > \overline{\alpha} \end{cases}.$$

K_c is a positive constant gain and e_c is the cross track error:

$$e_c = \tilde{x}\sin\psi_l - \tilde{y}\cos\psi_l,$$

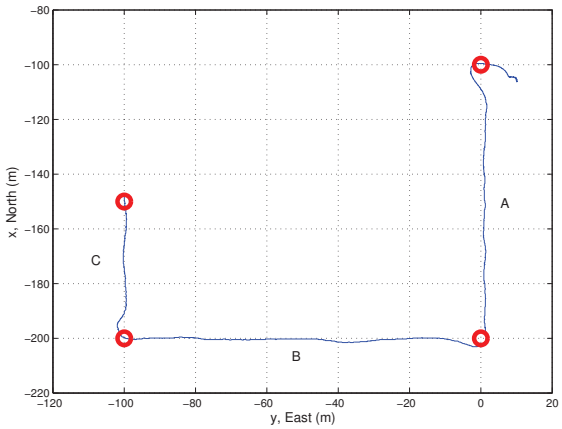

Fig. 3. Line-following trajectory. The waypoints are represented by the red circles. The initial waypoint is located at $[-100\ 0]^T$.

where

$$\begin{bmatrix}\tilde{x}\\ \tilde{y}\end{bmatrix} = \begin{bmatrix}x\\ y\end{bmatrix} - \begin{bmatrix}x_l\\ y_l\end{bmatrix},$$

with $[x_l\ y_l]^T$ being a point belonging to the line.

2) Target-tracking: Define the desired position in the earth-fixed coordinate system as $\eta_h^* = [x^*\ y^*]^T$ and the vehicle horizontal position as $\eta_h = [x\ y]^T$. The desired surge guidance law is chosen as a function of the distance to the target η_h^*:

$$u^* = K_d\left(||\eta_h^* - \eta_h|| - \delta\right), \tag{8}$$

with $K_d > 0$. Note that δ has been introduced to avoid the vehicle center of mass to coincide with the reference because of the well-known singularity in robots of this type (analog to the unicycle-like problem). See [7] for the unicycle singularity problem.

The desired yaw rate is chosen so that the vehicle points to the reference, obeying to the following guidance law

$$r^* = K_\psi e_\psi + \dot{\psi}_t, \tag{9}$$

with $K_\psi > 0$ being a gain constant. The angular error e_ψ is computed as

$$e_\psi = \psi_t - \psi$$
$$\psi_t = \text{atan2}(y^* - y, x^* - x).$$

V. Experimental results

Several missions have already been accomplished with the UCAP. The experimental results presented hereafter are the outcome of field trials to evaluate the performances of the vehicle and of its controllers while performing two basic maneuvers.

A. Line-following

A mission composed of four waypoints was designed. The lines to be followed by the UCAP are the segments between consecutive waypoints. Surge was set to $1\,\mathrm{m\,s^{-1}}$ and was estimated directly from GPS measurements, which naturally introduces errors as currents, wind and waves effects are not considered. However, assuming that the impact of such disturbances are small compared to the opposite forces and moments induced by the vehicle motion make it possible to neglect these effects for control purposes. The UCAP trajectory and the waypoints are depicted in Fig. 3. Over the operation, the vehicle was subjected to natural disturbances that impacted on the trajectory and on the cross-track error as it can be seen from Fig. 4, where it is noticeable that the first leg (up to $t = 139\mathrm{s}$) suffered a slightly greater cross-track error (in mean). Fig. 4 demonstrates that the vehicle is able to track the line with an error under $2\mathrm{m}$ with peaks slightly over $2\,\mathrm{m}$ when it changes from one line to another. These peaks are preceded by discontinuities that happen precisely when

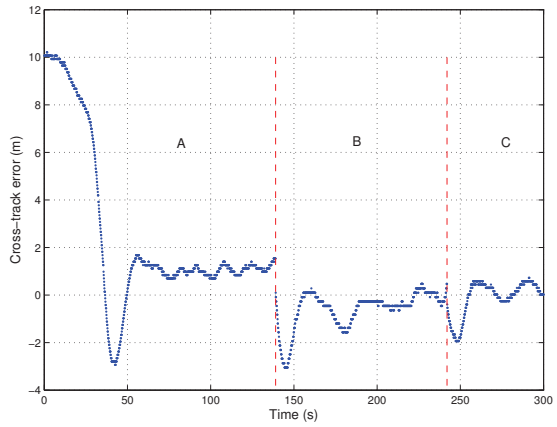

Fig. 4. Cross-track error

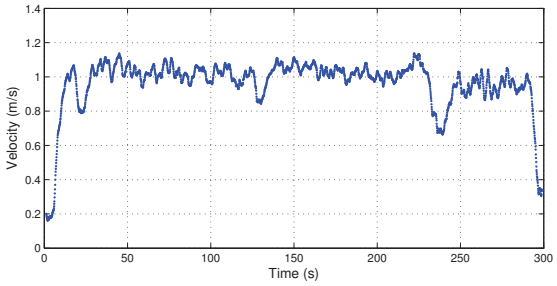

Fig. 5. Velocity

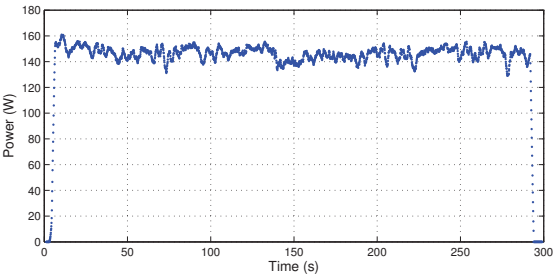

Fig. 6. Power consumption

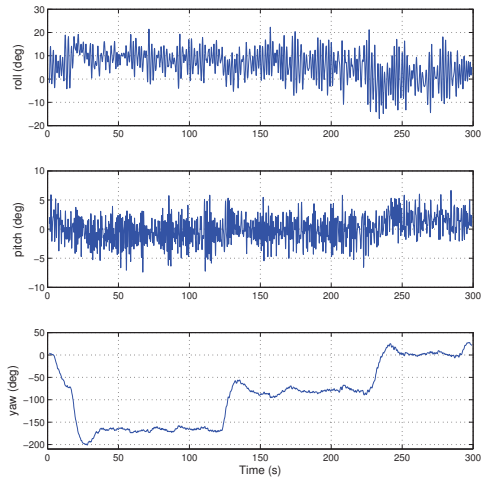

Fig. 7. Angles

there is a line change (when the waypoint is reached). The cross-track error appear to be positive on leg A and negative on leg B, after reaching steady state. The main cause of these errors are the disturbances, whose main contribution is given by the wind, which was observed to be predominantly from the south-west quadrant.

The velocity derived from GPS measurements over the mission is shown in Fig. 5, demonstrating that the vehicle was able to track the velocity reference. Power consumption is presented in Fig. 6, showing that the UCAP requires an average power of approximately $150\,\mathrm{W}$ to navigate at $1\,\mathrm{m\,s^{-1}}$. Fig. 7 depicts the vehicle attitude. Oscillation on roll and pitch are mainly caused by disturbances (mainly small waves), which appear to be more significant from $t = 150\mathrm{s}$ on.

B. Target-tracking

In order to evaluate the target-tracking guidance law performances, a path was set for a virtual reference (target) to follow. The path is derived from a cubic spline, on which the virtual reference slides. It should be noted that the evolution of the reference over the spline is dictated by the proximity of the vehicle, that is the distance between the vehicle and the reference. Therefore, unlike typical trajectory-tracking problems, the evolution of the reference position depends on the vehicle position. The reference path and the vehicle trajectory are depicted in Fig. 8. The reference and real trajectories appear to be very close, with an expected error in the longitudinal axis. Recall that the vehicle is expected to keep a non-null distance from the target, which was set to $\delta = 3\mathrm{m}$. The tracking distance was kept between 2 and $3.5\mathrm{m}$, with the offset to the desired distance being caused mainly by disturbances and modelling errors.

VI. Conclusions

The UCAP was designed to perform rescue mission at sea. The system was thought as an assembly of several modules, including power pack, electronics (computational system and sensors) and actuation. Control and guidance laws were derived and implemented in the on-board computer, enabling the UCAP to follow lines and track a dynamic target. Field trials were conducted and the results demonstrated the vehicle's capabilities and precision in positioning.

Acknowledgement

The research leading to these results has received funding from the European Union Seventh Framework Programme [FP7/2007-2013] under grant agreement number 285417, ICARUS project.

This work was partially funded by the project STRONGMAR - STRONGMAR: STRengthening MARritime technology Research Center (H2020-TWINN-2015 (CSA)-692427)

This work is financed by the ERDF – European Regional Development Fund through the Operational Programme for Competitiveness and Internationalisation - COMPETE 2020 Programme within project "POCI-01-0145-FEDER-00696", and by National Funds through the FCT – Fundação para a Ciência e a Tecnologia (Portuguese Foundation for Science and Technology) as part of project UID/EEA/50014/2013.

References

[1] *AGaPaS - Autonomous Galileosupported rescue vessel for persons overboard*, 2009.

[2] M. Patterson, A. Mulligan, and F. Boiteux, "Safety and security applications for micro-unmanned surface vessels," in *Oceans - San Diego, 2013*, Sept 2013, pp. 1–6.

[3] J. Alves and N. Cruz, "Fast - an autonomous sailing platform for oceanographic missions," in *OCEANS 2008*, Sept 2008, pp. 1–7.

[4] B. Ferreira, A. Matos, N. Cruz, and A. Moreira, "Coordination of marine robots under tracking errors and communication constraints," *Oceanic Engineering, IEEE Journal of*, vol. PP, no. 99, pp. 1–1, 2015.

[5] B. M. Ferreira, A. C. Matos, and N. A. Cruz, "Modeling and control of trimares auv," in *Robotica 2012: 12th International Conference on Autonomous Robot Systems and Competitions*, E. Bicho, F. Ribeiro, and L. Louro, Eds. Guimarães: Universidade do Minho, 2012, pp. 57–62.

[6] T. I. Fossen, *Guidance and control of ocean vehicles*. Wiley, 1994.

[7] E. D. Sontag, "Stability and stabilization: discontinuities and the effect of disturbances," in *Nonlinear analysis, differential equations and control*. Springer Netherlands, 1998, pp. 551–598.

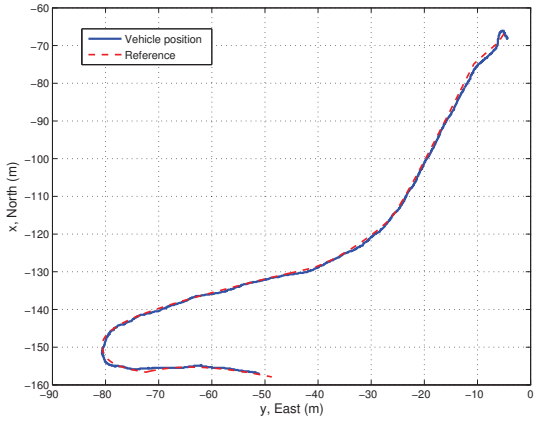

Fig. 8. Target-tracking trajectory